Journal of Thermal Analysis and Calorimetry, Vol. 67 (2002) 689–698

DIFFERENTIAL SCANNING CALORIMETRIC AND CIRCULAR DICHROISTIC STUDIES ON PLANT ANTIFREEZE PROTEINS

M. Lu[1*], *B. Wang*[1**], *Zh. Li*[1], *Y. Fei*[2], *L. Wei*[2] *and Sh. Gao*[2]

[1]Institute of Physical Chemistry, Peking University, Beijing 100871, P. R. China
[2]Institute of Developmental Biology, Chinese Academy of Sciences, Beijing 100080, P. R. China

(Received April 30, 2001; in revised form August 1, 2001)

Abstract

Antifreeze protein (AFP) can lower the freezing point by inhibiting the growth of ice crystals. In this article, the thermal hysteresis activity (THA) of a plant AFP was measured with differential scanning calorimetry (DSC). As is shown, when the amount of ice in the sample was less than 5% THA of this AFP reached as high as 0.35°C. The secondary structure of this AFP was studied with circular dichroism (CD). The CD spectrum from 195 to 240 nm indicated a well-defined secondary structure consisting 11% α-helix, 34% antiparallel β-sheet and 55% random coil.

Keywords: antifreeze protein, circular dichroism, differential scanning calorimetry, thermal hysteresis activity

Introduction

Antifreeze proteins (AFPs) are found in a variety of species, including fishes, insects, and, recently, plants [1–3]. In body fluid the function of AFPs is to inhibit the growth of ice crystal by binding to the surface of ice, and non-colligatively lower the freezing point (T_f). As a consequence, the freezing point is below the equilibrium melting point (T_m). The difference between T_f and T_m is defined as thermal hysteresis activity (THA), i.e. THA=T_m–T_f [1, 4]. In an equilibrium solution absent of AFP, the formation of an ice nucleus and further crystallization occur almost at the same time as the temperature drops. While in the presence of AFP, the ice-AFP interaction results in a delay in crystallization until the temperature is low enough to overcome the effect of AFP. Although the plant AFPs are in general much less effective than those found in fishes and insects [5], its profound effect on agriculture and other creatures on the earth still makes the studies on plant AFPs very important. Combined with biological

* Present address: Chem. Dept. of Univ. of Wisconsin, Madison, USA
E-mail: manchun@chem.wisc.edu
** Author to whom all correspondence should be addressed.

1418–2874/2002/ $ 5.00

Akadémiai Kiadó, Budapest
Kluwer Academic Publishers, Dordrecht

engineering, it might eventually be possible for a number of plant species to enhance the capability of enduring the threat of freezing in the wild.

THA is commonly measured with direct microscopic observation of crystal growth in a sample [4, 5]. The freezing point, a secondary onset temperature (T_o) of crystallization in a solution with an ice nucleus, is recorded by the observers' naked eyes. The ice fraction in the sample is roughly estimated according to the radii of the observed crystals based on an assumption that the actual ice crystal is ideal. Apparently, this method introduces in an observer-dependent problem and non-functional quantifiable assessment of ice fraction due to the discrepancy between real ice crystal and ideal crystal. In 1988, Hansen and Baust proposed a way to analyze the THA of fish AFPs, which were suspended in oil in the cell of differential scanning calorimeter (DSC) [4]. This method has been proved to be more accurate. The oil environment, however, is far different from the natural condition, which may have tremendous effect on the behavior of AFPs. On the basis of Hansen and Baust's method, we directly used aqueous solution of plant AFP and varied the experimental parameters to make this device more reliable, repeatable and suitable for studying plant AFPs system.

For any protein, the well-defined structure is a basis for its biological function. The secondary structure of fish AFPs has been extensively investigated with circular dichroistic (CD) spectroscopy [6, 7], NMR and X-ray crystallography [8]. At least four classes of macromolecules exist [1, 8, 9]: 1. antifreeze glycoproteins (AFGPs) consists of repeating tripeptide $(Ala\text{-}Ala\text{-}Thr)_n$ with a disaccharide attached to the threonyl residues; 2. AFPI is Ala rich (60%) and amphilic α-helix; 3. AFPII is the largest in the four types with relatively high content of Cys (8 mol%), five disulfide bridges and reverse turns; 4. AFPIII is mainly formed in β-sheet. Despite their distinct difference, all these AFPs interact with ice crystal in the same way by binding to the prism face of the ice crystal, therefore, becoming a barrier to further ice growth along α-axis [9–11]. To understand the mechanism of plant AFPs, the structural information of AFP at its natural state was obtained with CD spectrum, a useful and mature technique for structural study of biological macromolecules in solution.

Experimental

Materials

AFP from *Ammopiptanthus mongolicus* leaves was provided by Institute of Developmental Biology, Chinese Academy of Sciences. The improved Duman's method was used for the isolation and purification of AFP [2]. The six standard protein markers (phosphorylase b 94,000 D, albumin 67,000 D, ovalbumin 43,000 D, carbonic anhydrase 30,000 D, trypsin inhibitor 20,100 D and α-lactalbumin 14,400 D) were used to calibrate the SDS-PAGE. The molecular mass of this plant AFP was determined to be 22.96 KD. The concentration was 10 mg mL^{-1} for DSC experiment and 0.1 mg mL^{-1} for CD experiment.

Bovine serum albumin (BSA) was purchased from Sigma Chemical Co., MO, USA and directly used without further treatment. The concentration was 20 mg mL^{-1}. Water was twice distilled.

Apparatus and procedures

DSC experiment was performed on Micro DSCIII (SETERAM Co., France), which is designed particularly for biological and medical system. Temperature and baseline correction had been done with naphthalene before proceeding with all the experiments done in this study. BSA was used as a standard AFP-free solution in order to make a comparison between solutions with and without AFP. 3.5 μL sample was injected into the 1 mL sample cell and the reference cell was left empty. The sample was then cooled from 25 to –15°C at a rate of 1 K min^{-1}, frozen, and heated to totally melt (0.5 K min^{-1}). The enthalpy of melting (ΔH_m) was calculated from the DSC curve. The sample was then repetitively frozen at –15°C, followed by slowly heating (0.5 K min^{-1}) to a temperature at which the sample was not completely melted, containing a certain amount of ice crystal. To allow for ice-AFP interaction and system stabilization, the sample was held at this temperature (T_h, hold temperature) for 15 min before recooled at the same rate of 0.5 K min^{-1} to –15°C, during which the onset temperature (T_o) of crystallization was recorded and the exothermic enthalpy of refreezing (ΔH_r) was calculated. THA of AFP was defined as the difference between T_h and T_o, THA=T_h–T_o. The fraction of ice in the sample was estimated using $[1–(–\Delta H_r/\Delta H_m)]\cdot 100\%$. The experimental procedure above was repeated with different hold temperature so as to obtain different partially melted system with various ice-content.

CD spectroscopy was done using Jasca, J-500 spectropolarimeter with quartz cell of 0.2 cm path length at 15°C. CD spectrum was originally expressed in terms of absolute ellipticity (θ) in m° as a function of wavelength from 190 to 300 nm. Further analysis was completed with convex constraint analysis (CCA) using a mean residue mass of 114. The final results were CD spectra of five types of single secondary structure, in terms of molar ellipticity ([θ]) in deg cm^2 mol^{-1} as a function of wavelength from 195 to 240 nm. These types of single secondary structure included α-helix, β-turn, parallel β-sheet, antiparallel β-sheet and random coil, which could be recognized by the shape of CD band and [θ]. The fraction of these types of structure was also given with CCA.

Results

DSC measurements

DSC curves of freezing and melting process for BSA and AFP solutions are presented in Fig. 1. The sharp profile of their supercooling peaks at –12.17°C and –12.58°C, respectively, was very similar. However, the melting peak of BSA was comparatively narrow, only covering a temperature range of 2.6°C, whereas the melt-

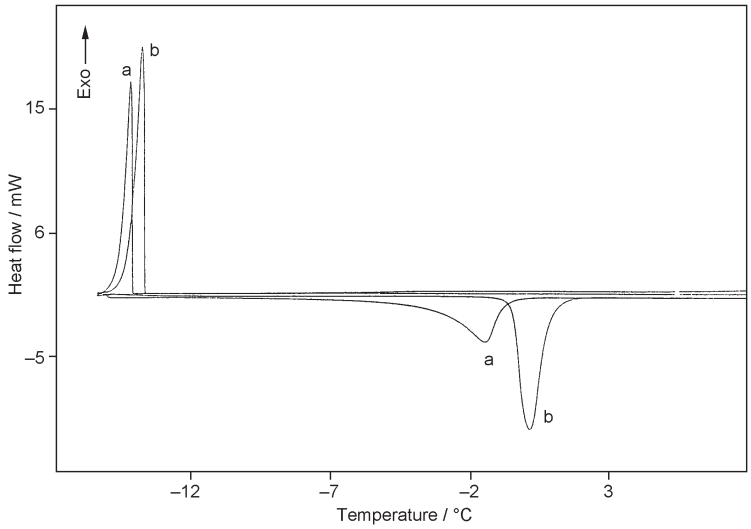

Fig. 1 DSC curves of freezing (1 K min^{-1}) and melting (1 K min^{-1}) process for a – AFP and b – BSA

ing peak of AFP was smooth and spread from –8.3 to 0°C. This result indicated that AFP might have stronger and more complicated interaction with ice-water system.

Frozen BSA was heated to partially melt at different hold temperature, and then cooled to recrystallize. Corresponding DSC curves and data are given in Fig. 2 and

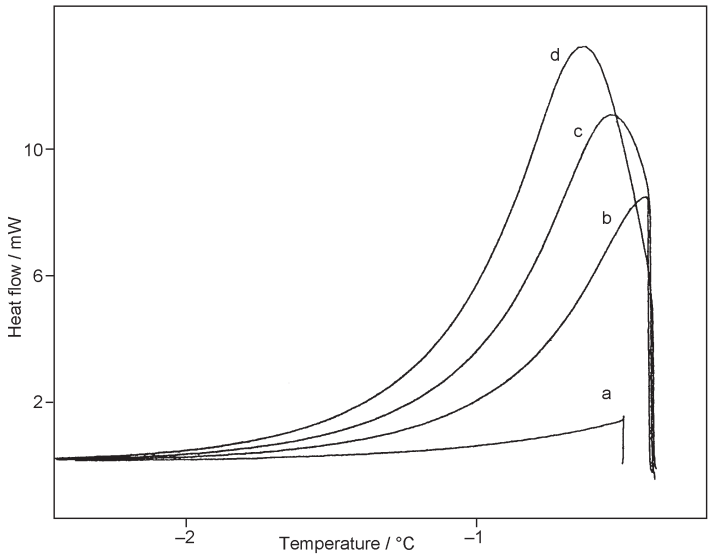

Fig. 2 DSC curves of refreezing (0.5 K min^{-1}) of partially melted BSA. The hold temperature (T_h) of the curves from a to d are –0.50, –0.40, –0.39, and –0.38°C, respectively. No thermal hysteresis effect was observed in each curve

Table 1 The hold and onset temperature (T_h and T_o), recrystallization enthalpy, ice fraction and THA of BSA

T_h/°C	–0.9	–0.8	–0.7	–0.6	–0.5	–0.4	–0.39	–0.38	–0.37
T_o/°C	–0.89	–0.79	–0.69	–0.59	–0.49	–0.4	–0.39	–0.38	–14.2
ΔH_r/J	–0.0588	–0.07	–0.0785	–0.1112	–0.1917	–0.8443	–1.1944	–1.1999	–1.2001
Nuclei/%	95	94	93	91	84	29	*	*	0
THA/°C	–0.01	–0.01	–0.01	–0.01	0.01	0	0	0	

Melting enthalpy ΔH_m=1.1943 J
Ice fraction=$[1–(–\Delta H_r)/\Delta H_m]\cdot 100\%$
*Due to the limit of instrument and the integral method, ice fraction less than 5% cannot be quantifiably calculated

Table 1. The area under the exothermic curves (a~d) increased with the increase of T_h from –0.50 to –0.37°C, indicating that the amount of ice nuclei in the equilibrium sample decreased accordingly. Recrystallization of the melted part started immediately after the temperature dropped, and the exothermic peak appeared without any delay. This indicated that the AFP-free BSA solution had no thermal hysteresis effect. When T_h rises to –0.37°C, the frozen BSA was completely melted, and the fluid sample refreezes at the supercooling point of –14.20°C.

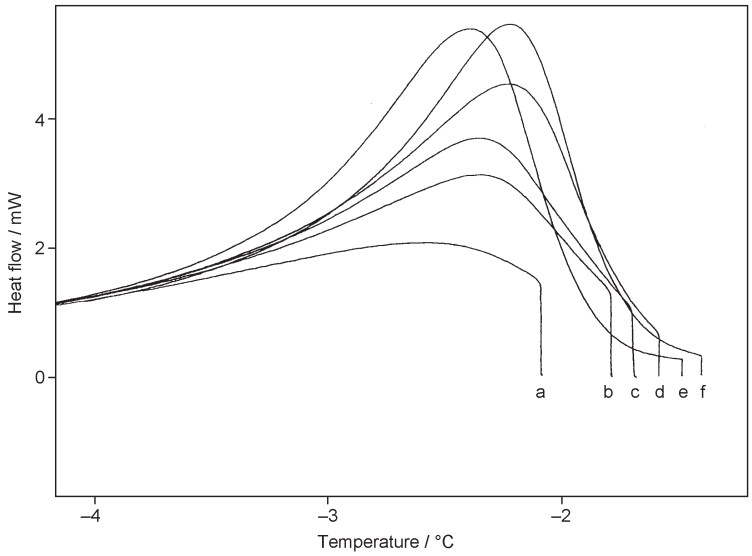

Fig. 3 DSC curves of refreezing (0.5 K min^{-1}) of partially melted AFP. The hold temperature (T_h) of the curves from a to f are –2.10, –1.80, –1.70, –1.60, –1.55, and –1.50°C, respectively. No thermal hysteresis effect was observed in curves a, b and c, whereas, THA of 0.03, 0.27 and 0.35°C was observed in curves d, e and f, respectively

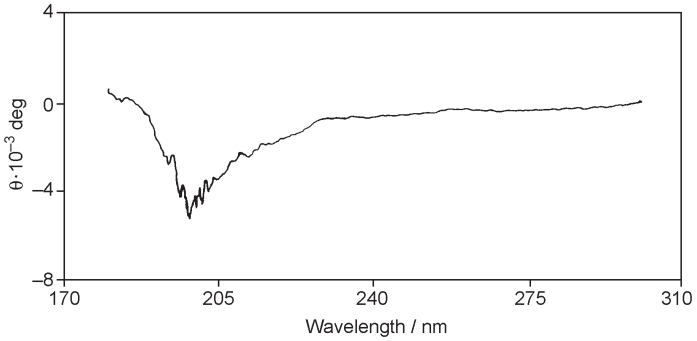

Fig. 4 Original CD spectrum of AFP at 15°C, wavelength range: 190~300 nm

Table 2 The hold and onset temperature (T_h and T_o), recrystallization enthalpy, ice fraction and THA of AFP

T_h/°C	–2.1	–1.8	–1.7	–1.6	–1.55	–1.5	–1.4
T_o/°C	–2.09	–1.79	–1.7	–1.63	–1.82	–1.85	–13.64
ΔH_r/J	–0.657	–0.8305	–0.8507	–0.9001	–0.9052	–0.906	–0.9101
Nuclei/%	27	8	5	*	*	*	0
THA/°C	–0.01	–0.01	0	0.03	0.27	0.35	

Melting enthalpy ΔH_m=0.8989 J
Ice fraction=$[1-(-\Delta H_r)/\Delta H_m]\cdot 100\%$
*Due to the limit of instrument and the integral method, ice fraction less than 5% can not be quantifiably calculated

DSC curves and corresponding data of the recrystallization of partially melted AFP system are presented in Fig. 3 and Table 2. Similarly, there was a decrease in ice fraction with increase in T_h. As T_h was within the range of –2.10~–1.70°C and the ice fraction was more than 5%, the recrystallization of partially melted AFP, very much like BSA, started without any delay as the temperature dropped, and the freezing peaks appeared immediately (a~c). When the ice fraction was less than 5%, however, a delay in the onset temperature of refreezing was observed to increase from 0.03 to 0.35°C as T_h increased from –1.60 (d) to –1.50°C (f), and the exothermic peaks appeared in a smoother manner. Compared to the DSC curves of BSA, AFP solution definitely showed some properties that were missing in BSA solution, the thermal hysteresis effect.

CD measurement

The original CD spectrum recorded from Jasca J-500 spectropolarimeter is shown in Fig. 4. The only negative CD band from 190 to 225 nm with a peak of $-5.30 \cdot 10^{-3}$ deg at 198.5 nm was within the characteristic region of α-helix (208 and 222 nm), β-sheet (215–218 nm) and random coil (194–198 nm). This band was likely to arise from a combination of these three structural types. In near-ultraviolet region (250–300 nm), the CD curve was almost flat and smooth without any obvious positive or negative band, indicating that no asymmetrically situated aromatic amino acid residues existed in the secondary structure of this plant AFP.

Further analysis of CD spectrum will be shown in the following discussion section (Fig. 4).

Discussion

Due to the interaction between AFP and ice nuclei, AFP solution showed an unusual property during melting process. Compared to BSA standard solution, AFP solution required longer time to get completely melted, and the exothermic peak was smoother (Fig. 1). According to the mechanism proposed for AFP's inhibiting ice-growth, it is reasonable to conclude that the bonding of AFP to ice nuclei can also affect the rate of melting, and most likely, in a negative manner.

Figure 3 clearly showed that when comparatively large amount of ice (>5%) existed in the system, the level of AFP accumulation was not high enough to suppress the ice growth as the temperature dropped. Explosive crystallization and the drop of temperature, therefore, were synchronistic. When the sample contained less ice (<5%) the freezing point of the partially melted AFP solution was considerably lowered. This condition is considered to be much closer to the initial natural phase when plants meet severe weather and start to freeze in the wild. Higher THA was observed with smaller ice fraction in the sample. This result was also in agreement with the proposed mechanism for AFP function.

A THA of 0.35°C observed here is higher than any other plant AFPs reported in previous literature, but is still lower than those found in fishes and insects. The degree

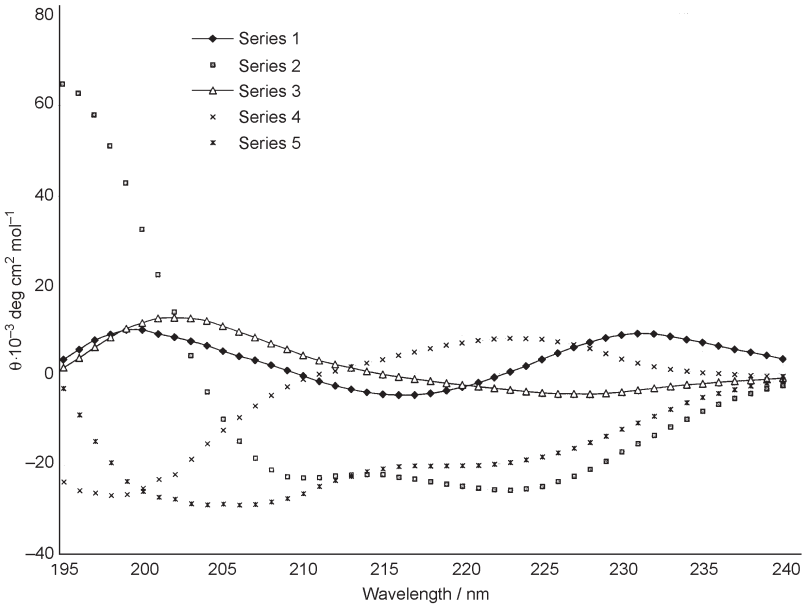

Fig. 5 Convex constraint analysis of CD data for AFP at 15°C, wavelength range: 195~240 nm. The single secondary structural types for each curve are (2) α-helix, (3) antiparallel β-sheet, (1, 4) random coil, (5) β-turn and parallel β-sheet. Combining these single structure result in a secondary structure of 11% α-helix, 34% antiparallel β -sheet and 55% random coil

of the lowered freezing point, however, is a comprehensive result from many antifreeze factors. In our experiments, the supercooling point of BSA solution was almost constant, ~–14.2°C, whereas the AFP's was apparently not repeatable (data not shown). This might be explained by the suggestion in some literature [12, 13] that AFPs also have the function of lowering the supercooling point. But the accuracy and mechanism of this proposed theory are still unresolved.

Secondary structure provides the most useful information for understanding the real mechanism of plant AFP. Further analysis of the CD spectrum shown in Fig. 4 was done using convex constraint analysis (CCA), shown in Fig. 5. The resultant CD band in far-ultraviolet region (195–240 nm), which contained the information of 'skeleton' structure for proteins, was resolved into five CD bands of single secondary structure. A mixed secondary structure of 11% α-helix, 34% antiparallel β-sheet and 55% random coil for AFP was also deduced from CCA. This structure, however, doesn't belong to any of the four existing secondary structures of AFPs found in deep-sea fish, indicating that the plant AFP might have some other unique structure different from those of fishes though they both have the capability of lowering freezing point. How does this structure actually function is still under investigation.

References

1 C. L. Hew and D. S. C. Yang, Eur. J. Biochem., 203 (1992) 33.
2 J. G. Duman, Biochimica et Biophysica Acta, 1206 (1994) 129.
3 W. C. How, M. Griffith, P. Chong and D. S. C. Yang, Plant Physiol, 104 (1994) 971.
4 T. N. Hansen and J. G. Baust, Biochim. Biophys. Acta, 957 (1988) 217.
5 J. G. Duman and T. M. Olsen, Cryobiology, 30 (1993) 322.
6 V. S. Ananthanarayanan, D. Slaughter and C. L. Hew, Biochim. Biophys. Acta, 870 (1986) 154.
7 D. Slaughter, G. L. Fletcher, V. S. Ananthanaryanan and C. L. Hew, J. Bio. Chem., 256 (1981) 2022.
8 F. D. Sonnichsen, B. D. Sykes, H. Chao and P. L. Davies, Science, 259 (1993) 1154.
9 P. L. Davies and C. L. Hew, FASEB J., 4 (1992) 2460.
10 A. L. Devries and Y. Lin, Biochim. Biophys. Acta, 495 (1977) 388.
11 D. Wen and R. A. Lausen, Biophys. J., 63 (1992) 1659.
12 J. G. Duman, J. Comp. Physiol. B, 131 (1979) 347.
13 J. G. Duman, J. Exp. Zool., 201 (1997) 333.